Tunneling spectroscopy of metal-oxide-graphene structure

Caifu Zeng,[a] Minsheng Wang, Yi Zhou, Murong Lang, Bob Lian, Emil Song, Guangyu Xu, Jianshi Tang, Carlos Torres, and Kang L. Wang
Department of Electrical Engineering, University of California, Los Angeles, California 90095, USA

(Received 19 March 2010; accepted 9 June 2010; published online 20 July 2010)

The unique density of states of graphene at the device level is probed via tunneling spectroscopy of macroscopic metal-oxide-graphene structures. Local conductance minima from electrons tunneling into the graphene Dirac point are observed in the dI/dV spectra of both the single-junction and dual-junction configurations. Nonequally-spaced Landau levels, including the hallmark n=0 level, are observed in the presence of a magnetic field. Linear energy-momentum dispersion near the Dirac point, as well as the Fermi velocity, is extracted from both experiments. Local potential fluctuations and interface defects significantly influence these fine physical features, leading to peak broadening and anomalies comparing to the results from the ultra sharp scanning tunneling microscope tip. This study provides important implications for potential tunneling-based graphene devices in the future. © *2010 American Institute of Physics*. [doi:10.1063/1.3460283]

Graphene has prompted great excitement and research efforts in both experimental and theoretical physics communities because of its fascinating physical properties arising from the unique band structure of this two-dimensional (2D) system.[1] The local density of states (DOS) of graphene has been widely studied by scanning tunneling microscopy (STM), which has revealed some interesting phenomena, including the phonon-assisted tunneling process, the impurity-induced disordered DOS, and the unique quantization of Landau levels (LLs) in the presence of a magnetic field.[2–8]

However, there are significant differences between the local DOS measured by an ultrasharp STM tip and the global DOS revealed by a macroscopic tunneling device, where the global DOS is the average of the local DOS within the whole junction area. As a realistic device, the metal-oxide-graphene (MOG) structure consists of a thin oxide layer as the tunneling barrier with a junction area up to microns. Interface states and defects introduced by the tunneling oxide have to be taken into consideration, as compared to the high vacuum in an STM system. In addition, spatial potential fluctuations (up to ~200 meV) (Refs. 8 and 9) over this relatively large junction area smear out some fine physical features, while reflecting the collective influences to the device. Little has been done on the tunneling spectroscopy of macroscopic MOG devices. So far other work has been limited to few-layer graphene devices, and they had a gate leakage problem at large bias voltage.[10]

In this paper, we present the tunneling spectroscopy of macroscopic MOG structures at various gate voltages and magnetic fields. Strikingly, a shift of the local conductance minimum in the gate-dependent dI/dV spectra for both the single-junction and the dual-junction configurations is observed, and this shift is attributable to electrons tunneling to the graphene Dirac point. Moreover, nonequally-spaced LLs, with the hallmark n=0 level, are also observed in the presence of a magnetic field. These fine physical features exist even in micron-scale devices but with broadened linewidth and some anomalies as compared to the STM spectroscopy.

The MOG structure is shown in Fig. 1(a). The graphene flakes were prepared by mechanical exfoliation on a highly doped Si substrate with 300 nm thick thermally grown SiO_2. The thickness of the flake was identified through optical microscopy and Raman spectroscopy.[11] Two metal electrodes, B1 and B2, used for contacts onto graphene were patterned by E-beam lithography followed by Ti/Au evaporation. Subsequently, 1.2 nm thick aluminum was deposited on top of graphene by E-beam evaporation at room temperature and then oxidized into Al_2O_3. The estimated thickness of the Al_2O_3 is less than 2 nm, and pinholes are usually inevitable at this thickness. However, the main physical phenomena associated with tunneling transport are usually still observable in the electrical measurement with Al_2O_3 thickness down to around 2 nm.[10,12] Finally, another two electrodes, T1 and T2, used as the M region in the MOG junction, were patterned and deposited by the same method as used for B1 and B2.

For every device, two-terminal conductance was first measured upon B1 and B2 to make sure the contacts between the electrodes and the graphene are Ohmic with the dc bias up to 300 mV. The differential conductance between B1 and B2 as a function of gate bias was also measured, from which the mobility of the graphene sheet was extracted. For most of our samples, the mobility ranges from 3000–6000 $cm^2\ V^{-1}\ s^{-1}$, depending on the quality of the graphene, and this range is comparable to that of samples without Al_2O_3 on top.

The tunneling spectroscopy experiments were performed at low temperatures from 2 to 100 K in a commercial physical property measurement system manufactured (PPMS) by Quantum Design. Figure 1(a) also shows the diagram of the experimental setup. A dc bias V_B was applied to the top metal electrode, on which a root mean square modulation voltage of 1 mV at a frequency of 1 kHz was superimposed. The differential conductance was directly measured by using a Stanford Research SR530 lock-in amplifier with a reference frequency of 1 kHz, and the gate bias was applied by a

[a]Electronic mail: czeng@ee.ucla.edu.

 © 2010 American Institute of Physics

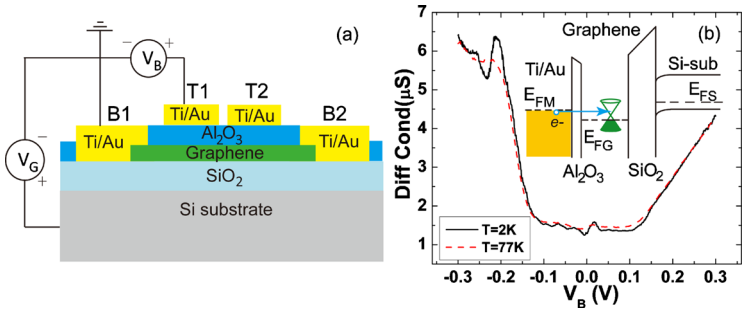

FIG. 1. (Color online) (a) The cross-section of the MOG structure. The circuitry shows one of the experiment setups. (b) The typical dI/dV spectra of the MOG structure measured at $T=2$ K (solid line) and $T=77$ K (dashed line). (Inset: the band diagram of the MOG junction).

Keithley 2400 source-meter. The band diagram of the MOG structure is shown in the Fig. 1(b) inset.

The minimum conductance in the dI/dV spectra of the MOG structure measured at $T=2$ and 77 K at zero gate bias without the presence of a magnetic field shows a very weak temperature dependence [Fig. 1(b)], which confirms that the electric current is dominated by the tunneling process instead of thermally activated hopping through pin-holes or defects. The dI/dV spectra were also measured at various gate bias ranging from −50 to 50 V [Fig. 2(a)]. The changing of the gate bias causes the shift of the Dirac point of graphene E_D relative to the graphene Fermi level E_{FG}, inducing a two dimensional carrier density of $n_s=\alpha(V_G-V_{Dirac})$, where α is 7.1×10^{10} cm^{-2} V^{-1} for 300 nm SiO_2 substrate based on a simple capacitor model.[1,13] A set of local conductance minima are observed to shift monotonically with the gate bias [arrows in Fig. 2(a)], which is consistent with previous STM experiments.[5] The gate-dependent conductance minima are attributable to electrons tunneling to the graphene Dirac point, where the DOS of graphene reaches the minimum.[14] These conductance minima shift as the Dirac point of graphene relative to E_{FG} is modulated by the gate bias.

The origin of the conductance minima can be also confirmed by applying the voltage bias between T1 and T2. In this configuration, the two MOG junctions are in series. Two gate-dependent local conductance minima are observed in the dI/dV spectra, as shown in Fig. 2(b). The explanation is straightforward: At positive bias voltage, the tunneling of electrons into the Dirac point through one of the MOG junctions creates a first conductance minimum on the right; at negative bias voltage, the tunneling of electrons into the Dirac point through the other MOG junction creates a second conductance minimum on the left. This dual-junction tunneling spectrum is unique for the MOG structure, since the prior STM experiments were not able to provide two tips on one graphene flake at the same time.[5,8]

The identification of the conductance minima can be further confirmed by fitting their energy positions with the expected dependence, $E=\hbar v_F\sqrt{\pi\alpha(V_G-V_{Dirac})}$ in the vicinity of the Dirac point.[14] As shown in the inset of Fig. 2(a), a linear fitting can be obtained from plotting the measured bias voltages of the conductance minima, V_D, as a function of the calculated graphene Dirac point energy, E_D, relative to the graphene Fermi level, E_{FG}. This fitting confirms the low energy dispersion around the graphene Dirac point is linear.[13] The Fermi velocity $v_F\sim1.64\times10^6$ ms^{-1} is extracted from the slope of this fitting, which is larger than the prior STM experiment results.[3–5] The origin of this difference is not clear yet; it might come from the electron-phonon coupling,[4] or the energy shift caused by local potential fluctuations within the junction area.[8,9]

Moreover, the shape of the dI/dV spectrum changes significantly as the gate bias is varied. Small peaks near $V_B=0$ [circled in Figs. 1(b) and 2(a)] appear at 2 K and smear out at 77 K with no gate dependence. These fine features are believed to come from the impurities on graphene within the

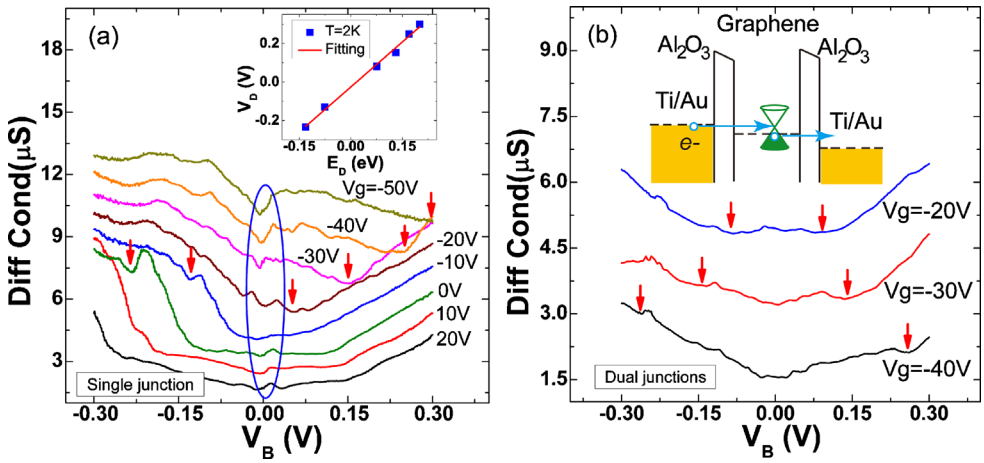

FIG. 2. (Color online) (a) Gate-modulated tunneling spectra of the MOG structure with the back gate voltage ranged from −50 to +20 V at $T=2$ K. The curves are offset by 1 μS for clarity. Arrows indicate the local conductance minima caused by electrons tunneling into the graphene Dirac point. The circled small peaks near the zero bias are possibly from electrons tunneling to disordered states or interface defects.(See Ref. 6) [Inset: the positions of the conductance minima as a function of the Dirac point energy relative to the graphene Fermi level E_{FG} calculated from the capacitor model (See Ref. 1)]. (b) The dI/dV spectra of two MOG junctions in series at different gate voltages. The arrows at the positive bias and the negative bias indicate two conductance minima coming from electrons tunneling into the Dirac point through each junction. (Inset: the band diagram of dual-junction configuration).

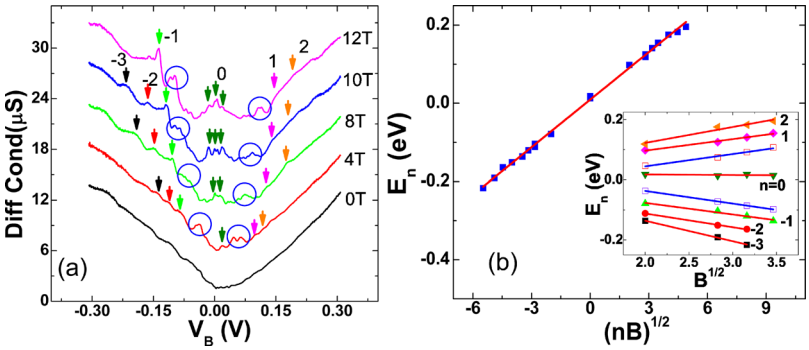

FIG. 3. (Color online) (a) The dI/dV spectra of the MOG structure in the presence of various perpendicular magnetic fields from 0 to 12 T at $T=2$ K. Arrows indicate the well-defined, nonequally spaced LLs that follow the linear dependence on $\sqrt{nB}$. The circles indicate abnormal peaks that appear between n=0 and 1 levels. The curves are offset for clarity. (b) The LL energy E_n vs $\sqrt{nB}$. The linear fitting shows the LL energy is proportional to $\sqrt{nB}$. (Inset: LL energy E_n vs $\sqrt{B}$ for each index n. Solid dots represent the peaks follow the linear dependence on $\sqrt{nB}$; Open dots represent the abnormal peaks appear between n=0 and 1 levels).

junction area, which induce disordered DOS in graphene, especially in the low energy region.[6,15]

Tunneling spectroscopy experiments were also performed in the presence of various magnetic fields (from 0 to 12 T) perpendicular to the MOG interface at $T=2$ K. A couple of conductance peaks are pronounced in the dI/dV spectra as the magnetic field increases [labeled in Fig. 3(a)], and these peaks are attributable to electron and hole states condensing into LLs in a magnetic field. Owing to graphene's unique linear energy dispersion relation, these LLs have a square-root dependence on both the field B and the LL index n, as in $E_n=\mathrm{sgn}(n)\sqrt{2e\hbar v_F^2|n|B}$ n $=0,\pm1,\pm2,\ldots$, as well as the hallmark n=0 LL, which is different from the equally spaced LLs in normal 2D electron gas.[3,4]

By fitting the LLs energy, E_n, as a function of $\sqrt{|n|B}$, the Fermi velocity of 1.1×10^6 ms^{-1} with Dirac point energy 10 meV above the Fermi level is extracted [Fig. 3(b)]. The velocity value is consistent with previous studies,[3,4,7] illustrating that the tunneling process and LLs across the junction area is fairly homogeneous, although the linewidth of the peaks is not as sharp as that observed in the STM experiments. The broadening is caused by averaging the local potential fluctuations within the macroscopic MOG junction area.

The distinct n=0 LLs of graphene are also observed in the dI/dV spectra of the MOG device near the graphene Dirac point [Fig. 3(a)]. More than one peak appears with a small energy difference. Those peaks could come from the splitting of the n=0 level into 0+ and 0−, which can be attributed to the broken sublattice symmetry, as the splitting occurs at the Dirac point rather than the Fermi level.[3,4] It is also possible that the potential fluctuations of graphene across the junction area create more than one peak at different spatial locations with a small potential shift, which leads to multiple peaks that belong to the same index number n.

Similar phenomena were also observed for n=1 LLs. Two extra sets of peaks with energies between the well-defined n=0 and 1 LLs are observed in the dI/dV spectra [circled in Fig. 3(a)]. Their peak positions are also proportional to $\sqrt{B}$, and their LL index, n, extracted from the slopes of the linear fitting, is equal to 1 [inset of Fig. 3(b)]. Therefore, the origin of these two sets of peaks also comes from the potential fluctuations within the whole junction area, which shift the n=1 LLs at different spatial locations to form the extra peaks in dI/dV spectra.

In conclusion, the tunneling spectroscopy of the macroscopic MOG structure has been studied at various gate voltages and magnetic fields. Even though the interface defects and potential fluctuations are usually unavoidable and lead to some unexpected peaks and broadened linewidth, as compared to the STM spectroscopy, fine physical features are preserved even when the device size is of micron-scale, suggesting the tunneling process associated with the DOS of graphene is fairly homogeneous. The direct probe of graphene's unique DOS via tunneling spectroscopy of realistic macroscopic devices provides important implications for potential tunneling-based graphene devices in the future, such as the tunneling hot-electron transistor.[16]

The authors would like to acknowledge Professor H. W. Jiang and Dr. M. Xiao at UCLA for providing us access to the E-Beam lithography facility and Professor W. Beyermann, Dr. Z. Yang, and J. R. Morales at UC Riverside for providing us access to the PPMS. This work was in part supported by Functional Engineered Nano Architectonics (FENA).

[1]K. S. Novoselov, A. K. Geim, S. V. Morozov, D. Jiang, Y. Zhang, S. V. Dubonos, I. V. Grigorieva, and A. A. Firsov, Science **306**, 666 (2004).
[2]Victor W. Brar, Sebastian Wickenburg, Melissa Panlasigui, Cheol-HwanPark, Tim O. Wehling, Yuanbo Zhang, Régis Decker, Ã‡aÄŸlar Girit, Alexander V. Balatsky, Steven G. Louie, Alex Zettl, and Michael F. Crommie, Phys. Rev. Lett. **104**, 036805 (2010); S. Nie and R. M. Feenstra, J. Vac. Sci. Technol. A **27**, 1052 (2009); T. Matsui, H. Kambara, Y. Niimi, K. Tagami, M. Tsukada, and Hiroshi Fukuyama, Phys. Rev. Lett. **94**, 226403 (2005).
[3]D. L. Miller, K. D. Kubista, G. M. Rutter, M. Ruan, W. A. de Heer, P. N. First, and J. A. Stroscio, Science **324**, 924 (2009).
[4]G. Li, A. Luican, and E. Y. Andrei, Phys. Rev. Lett. **102**, 176804 (2009).
[5]Y. B. Zhang, V. W. Brar, F. Wang, C. Girit, Y. Yayon, M. Panlasigui, A. Zettl, and M. F. Crommie, Nat. Phys. **4**, 627 (2008).
[6]G. M. Rutter, J. N. Crain, N. P. Guisinger, T. Li, P. N. First, and J. A. Stroscio, Science **317**, 219 (2007).
[7]G. Li and E. Y. Andrei, Nat. Phys. **3**, 623 (2007).
[8]V. W. Brar, Y. Zhang, Y. Yayon, T. Ohta, J. L. McChesney, A. Bostwick, E. Rotenberg, K. Horn, and M. F. Crommie, Appl. Phys. Lett. **91**, 122102 (2007).
[9]J. Martin, N. Akerman, G. Ulbricht, T. Lohmann, J. H. Smet, K. von Klitzing, and A. Yacoby, Nat. Phys. **4**, 144 (2008).
[10]N. Staley, H. Wang, C. Puls, J. Forster, T. N. Jackson, K. McCarthy, B. Clouser, and Y. Liu, Appl. Phys. Lett. **90**, 143518 (2007).
[11]A. C. Ferrari, J. C. Meyer, V. Scardaci, C. Casiraghi, M. Lazzeri, F. Mauri, S. Piscanec, D. Jiang, K. S. Novoselov, S. Roth, and A. K. Geim, Phys. Rev. Lett. **97**, 187401 (2006).
[12]Yi Zhou, Masaaki Ogawa, Xinhai Han, and Kang L. Wang, Appl. Phys. Lett. **93**, 202105 (2008); N. Tombros, C. Jozsa, M. Popinciuc, H. T. Jonkman, and B. J. van Wees, Nature (London) **448**, 571 (2007).
[13]K. S. Novoselov, A. K. Geim, S. V. Morozov, D. Jiang, M. I. Katsnelson, I. V. Grigorieva, S. V. Dubonos, and A. A. Firsov, Nature (London) **438**, 197 (2005).
[14]A. H. Castro Neto, F. Guinea, N. M. R. Peres, K. S. Novoselov, and A. K. Geim, Rev. Mod. Phys. **81**, 109 (2009).
[15]Ben Yu-Kuang Hu, E. H. Hwang, and S. Das Sarma, Phys. Rev. B **78**, 165411 (2008).
[16]M. Heiblum, Solid-State Electron. **24**, 343 (1981).